Substrate Integrated Waveguide H-Plane Horn Antenna with Symmetric Beamwidths

Farzeen Iqbal, Jens Bornemann
Department of Electrical and Computer Engineering, University of Victoria
Victoria, BC, V8W 3P6, Canada

Abstract—A substrate integrated waveguide (SIW) H-plane horn antenna with approximately symmetric beamwidths in both E- and H-planes is proposed. Radiation patterns are analyzed and to validate simulation results, measurements are performed on a fabricated prototype antenna. To obtain a narrower half-power beamwidth in both E- and H-planes, two rectangular slots are inserted in the top metallization which radiate the field at an angle from the horizontal, presenting an approximately symmetric main beam. The measured half-power beamwidths at 26.3 GHz are 35° and 22° in the E- and H-planes, respectively, with a gain of 11.6 dB and a 10-dB return loss bandwidth of 600 MHz (4.6 %).

Keywords—Substrate integrated waveguide (SIW); horn antenna; HPBW; coaxial feed.

I. INTRODUCTION

For the evolution of RF systems, the implementation of millimeter-wave) integration technology is pivotal and primarily depends on the availability of a cost-effective solution, suitable for mass production. To realize this objective, substrate integrated waveguide (SIW) technology [1] presents itself as the most viable solution within the family of substrate integrated circuits [2]. Like planar circuits, SIW structures are compact, light-weight, easy to fabricate and cost effective. They also preserve some of the major advantages of metallic waveguides, namely, low loss, high quality factor and high power handling capabilities [1].

For applications in RF systems, several SIW planar horn designs have been proposed over the last decade. For instance, a compact H-plane substrate integrated waveguide horn antenna design [3] promises better antenna directivity using a dielectric arc lens and microstrip feed. In [4] a dielectric loaded millimeter-wave H-plane horn antenna using low-temperature co-fired ceramic (LTCC) technology is proposed. Another design for radar application in the 21 - 28 GHz frequency range is proposed in [5]; it utilizes a PTFE substrate and presents an increase in gain and narrower H-plane and E-plane beamwidths. In a recent study [6], the authors propose a uniform aperture distribution for an H-plane SIW horn antenna. In [7] an improved E-plane radiation pattern from a coaxial-fed dual-layer SIW horn antenna is demonstrated. This antenna has a 10-dB bandwidth of 5.37 percent and a gain of 10.33 dB at 21.5 GHz. An approach like the one in this paper had been proposed in [8] where two square loop slots were introduced in an H-plane horn antenna to maximize bandwidth and gain; a two slots design achieves a maximum bandwidth of 800 MHz at 21.4 GHz. However, measurements are not provided.

Therefore, this paper proposes a new design with two rectangular slots etched in the top metallization. Fig. 1 shows the front and back of the proposed SIW H-plane horn antenna design. Approximately symmetric half-power beamwidths in both E- and H-planes along with higher gain is obtained.
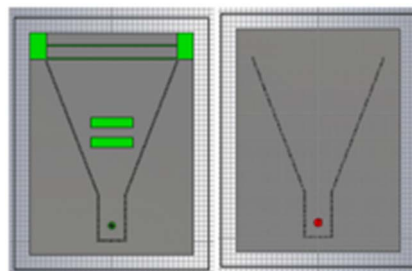

Fig. 1: Slotted substrate integrated waveguide H-plane horn antenna; front (left) and back (right).

II. DESIGN PROCEDURE

This section discusses the design of the slotted substrate integrated waveguide H-plane horn antenna in detail. Four stages are presented: first, a simple SIW H-plane horn antenna; second, the addition of rectangular slots in the top metallization; third, the extension of the ground plane; and fourth, parallel plate transitions for front-to-back ratio enhancement.

In general, the design commences with the selection of the substrate, via diameter, via separation, and waveguide width. The substrate material is selected as RT/Duroid 5870 with dielectric constant of 2.33 and thickness h = 1.575 mm. The via-hole diameter of (1/64)" and via separation of 0.6 mm fall within the range of $0.5 < d/p < 0.83$ as proposed in [9].

Step 1: SIW horn antenna: For a given equivalent waveguide width a_{eq} of 4.9037 mm (SIW width of 5.2 mm), a simple substrate integrated waveguide H-plane horn antenna is designed for a cutoff frequency of f_c = 20 GHz and initial gain of 9 dB. Once the simulation of this SIW horn antenna is run in CST Microwave Studio, the E- and H-plane radiation patterns are obtained as shown in Fig. 2. At 26.3 GHz, a gain of 8.2 dB is obtained with H- and E-plane half-power beamwidths of 30° and 126°, respectively. We can see that the beamwidth in the E-plane is much wider than that in the H-plane.

Step 2: Addition of slots: Now, to achieve symmetric beamwidths in both E- and H-planes, two rectangular slots are inserted in the top metallization. These two slots radiate the field at an angle of 57° from the horizontal, resulting in a narrower main beam of 28° in both E- and H-planes. The rectangular slots are inserted with an offset of λ/2 between them, each slot has a

width of $\lambda/4$. The distance between the slots is kept as $\lambda/2$, such that the slots will be fed in phase which is an equivalent electrical spacing of 180°. Therefore, each slot is exactly out of phase with its neighbor so that their radiations cancel. This results in a main beam which is inclined from the horizontal. For the position of the first slot (the one closest to the source), the center of the slot is kept at a quarter wavelength away from the closed end of the waveguide. Since a short-circuited quarter wavelength stub works as an open-circuit, the closed end does not impact on the impedance. However, in this case the start position is determined by $m \times \lambda/4$, where m is selected and optimized to obtain the desired radiation pattern. Note that the number of slots in the top metallization was varied from two to four. It was observed that any number of slots greater than two resulted in higher side lobe level in the E-plane and poor front-to-back ratio. Therefore, this paper discusses only the two-slot design. Fig. 3 shows the radiation patters obtained from the slotted SIW H-plane horn antenna.
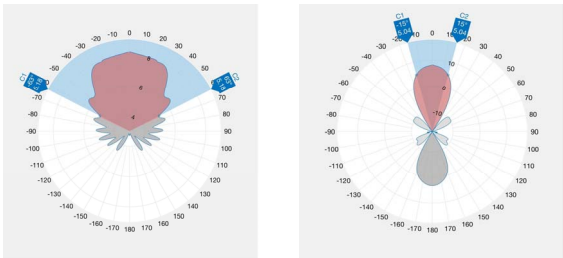

(a)   E-plane   (b) H-plane
Fig. 2. Radiation patterns of simple SIW H-plane horn antenna.
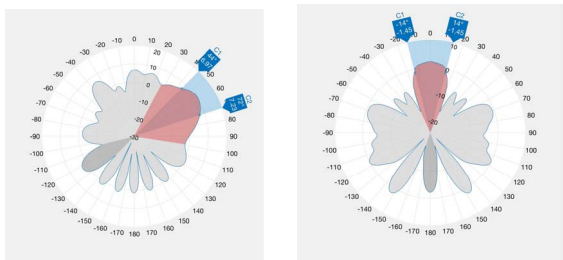

(a)   E-plane   (b) H-plane
Fig. 3. Radiation patterns of a slotted SIW H-plane horn antenna.

TABLE I Performance comparison of the SIW horn antennas with and without slots

Parameter	Without Slots	With Slots
Gain	8.2 dB	10.4 dB
Beamwidth (H)	30°	28°
Beamwidth (E)	126°	28°
Front-to-back ratio (H)	4.92 dB	4.29 dB
Front-to-back ratio (E)	4.92 dB	7.37 dB
Side lobe (H)	4.92 dB	0.088 dB
Side lobe (E)	2.74 dB	3.49 dB
Direction of the main beam	0°	57°

Table I compares the results between both SIW horn antennas with and without rectangular slots. We observe a considerable increase in the gain when the slots are inserted in

the top metallization along with a resulting main beam inclined from the horizontal.

Step 3: Extension of ground plane: For more radiation directed towards the main lobe, measures can be taken to enhance the front-to-back ratio. To achieve this objective, the ground plane is extended up to the end of the substrate. This allows the field to travel farther in the substrate, reducing the back-lobe. It also reduces the radiation at the edge of the metallization, thereby enhancing the front-to-back ratio. Fig. 4 depicts the radiation patterns obtained when the ground plane is extended.

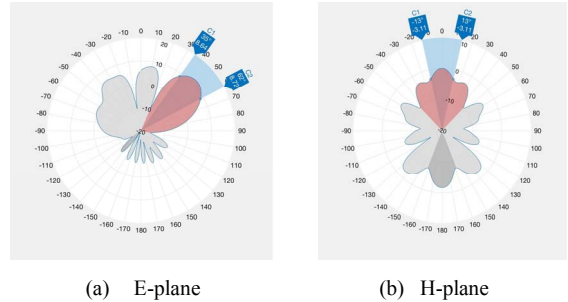(a)   E-plane   (b) H-plane
Fig. 4. Radiation patterns of slotted SIW H-plane horn antenna with ground extension.

We observe that in the E-plane, the main lobe level increases significantly, from 10.4 dB to 11.9 dB, the back-lobe level reduces to -9.99 dB from 2.99 dB and the front-to-back ratio increases comparably to 21.8 dB from 7.37 dB, without significantly affecting the main lobe beamwidths in the two planes. However, an increase in the side lobe level is observed.

Fig. 5 compares the 10-dB return loss bandwidths obtained from simulations at the three stages of the design over a wide range of frequencies. The blue line represents S_{11} for a simple SIW H-plane horn antenna, red represents S_{11} for the horn with two rectangular slots, and yellow represents the slotted SIW horn with ground extension.
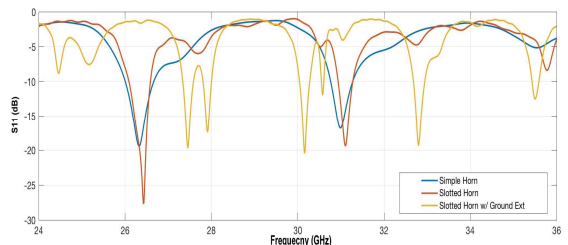

Fig. 5. Comparison of reflection coefficient at three stages of the design.

The S_{11} curve for a simple SIW H-plane horn antenna represents narrow bandwidth at frequencies of 27.5, 30.2 and 32.8 GHz. The S_{11} curve for the horn with two rectangular slots (symmetric beamwidths) is shown in red. We observe that the S_{11} level considerably improves with a lower number of bands over the plotted frequency range. The results with extended ground plane indicate much greater improvement in the front-to-back ratio but at the cost of reduced S_{11} level, represented by the yellow curve in Fig. 5. In all three stages, the bandwidth remains narrow due to a mismatch between the edge of the dielectric slab and air.

Step 4: Parallel plate transitions: To achieve a good compromise between symmetric beamwidth and wider bandwidth, a printed transition consisting of two parallel plates/directors is implemented similar to [10]. The authors propose a transition etched in the same dielectric substrate as that of the antenna; the working principle of these transitions is that of parallel-plate resonators separated by distance s. The length of the transition can be calculated from [11].

$$\frac{2\pi L}{\lambda_0} + \beta_{pp} L = (2\eta + 1)\pi \qquad \eta \epsilon Z \qquad (1)$$

and

$$\beta_{pp} = \frac{2\pi \sqrt{\varepsilon_{rpp}}}{\lambda_0} \qquad (2)$$

β_{pp} is the propagation constant of the parallel plate waveguide, and ε_{rpp} can be calculated from the quasi-static approximation presented in [12]. The resonant frequency of one block is

$$f_{r1} = \frac{c}{2L_{eq}\sqrt{\varepsilon_r}} \qquad (3)$$

where L_{eq} is an equivalent length determined by

$$L_{eq} = L(1 + \frac{0.7h}{L}) \qquad (4)$$

The resonant frequency stated above shifts when two or more blocks are implemented. This is due to the fact that the coupling effect enhances and reduces the ability of a single block to store the charge. Since the blocks are separated by spacing s, two resonant frequencies, $f_{r2-} < f_{r1}$ and $f_{r2+} > f_{r1}$ are generated. A coupling factor k_2 is used to calculate f_{r2}.

$$f_{r2} = \frac{f_{r1}}{\sqrt{1 + k_2}} \qquad (5)$$

Details of how to calculate k_2 are presented in [11]. After optimizing the values obtained from these equations, the gap between the plates is $s_0 = 0.189$ mm, and the length of the plates is $L_{eq} = 2.45$ mm each. The transmission zeros in the antenna's reflection coefficient represent the number of parallel plate transitions. Since the length of both plates is the same, this should result in a single transmission zero at resonant frequency. The two transmission zeros appearing in Fig. 6 are due to the fact that the plate's transition is only located in the top plane of the substrate, whereas at the bottom, the antenna has an extended ground plane.
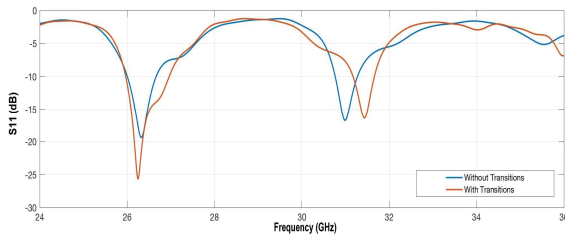

Fig. 6. Comparison of return loss with and without transition.

The 10-dB return-loss bandwidth improves from 600 MHz without transitions to 1 GHz with transitions, and the reflection coefficient improves to 25.6 dB from 18 dB at 26.3 GHz. There is a slight variation in the beamwidths of the E- and H-planes, they are now 33° and 22°, respectively, as shown in Fig.7.

Moreover, a slight reduction in the gain from 11.9 dB to 11.6 dB is observed. But overall a reasonable compromise is achieved with narrow beamwidths in both planes and improved bandwidth.
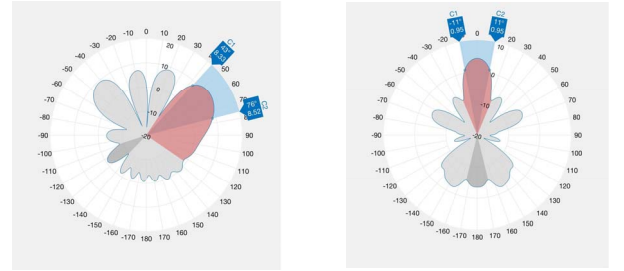
(a) E-plane   (b) H-plane
Fig. 7. Radiation patterns of slotted SIW H-plane horn antenna with printed transition.

The final dimensions of the SIW H-plane horn antenna with approximately symmetric beamwidths are displayed in Table II.

TABLE II Dimensions of slotted SIW H-plane horn antenna

Parameter	Dimensions (mm)
Horn aperture	25.5952
Equivalent waveguide width	4.9037
SIW width	5.2
Diameter of vias	0.396875 = 1/64 "
Substrate height	1.575
Via separation (pitch)	0.6
Length of horn flare	26.3351
Offset (b/w slots)	3.9307
Width of the slots	1.96535
Length of the slots	8.3168
Position of the first slot	18.7176

III. MEASUREMENTS

Fig. 8 shows the front and back views of the antenna prototype. Fig. 9 compares measured and simulated reflection coefficients. The blue solid line indicates the simulated results over the frequency range of 25 - 28 GHz, whereas the red dashed line represents the measured results. The simulations show a 10-dB return-loss bandwidth of 1GHz, i.e., 8.46 % and a reflection coefficient of 26 dB at 26.3 GHz. According to the measurement, a bandwidth of approximately 600 MHz (4.62 %) with a reflection coefficient of 25.02 dB at 26.3 GHz is obtained. However, the general shape of the reflection coefficient over frequency is reproduced. The difference is attributed to the coaxial connector and soldering when in CST, the coax connector is modeled as a perfect electric conductor.

Fig. 10 shows the measured far field radiation patterns. We observe that in the E-plane, the measured half-power beam-width (HPBW) at 26.3 GHz is 35° which agrees with the beam-width of 33° obtained from simulation; similarly, the H-plane HPBW is measured to be 20° as compared to 22° obtained from simulations. The main beam is directed at an angle of 55° from the horizontal, which agrees with the direction of the main beam from simulated results.

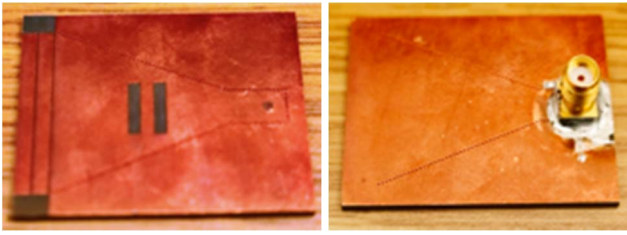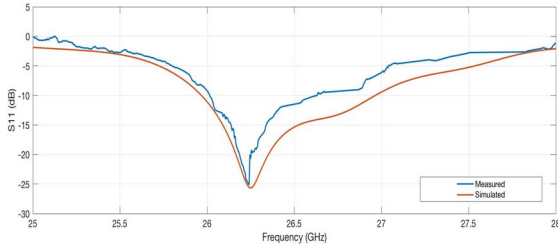Fig. 8. Front (left) and back (right) views of the prototype antenna.
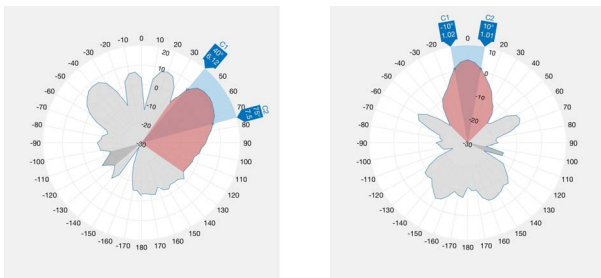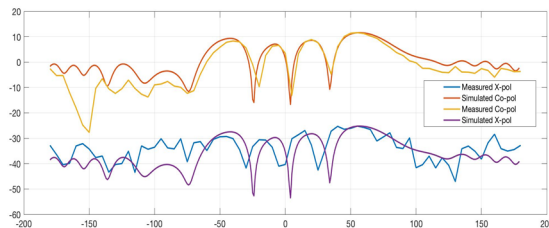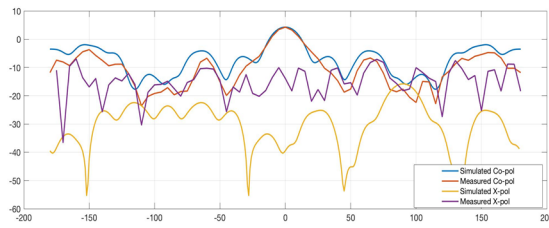

Fig. 9. Comparison of measured and simulated return loss.

(a) E-plane   (b) H-plane
Fig. 10. Measured radiation patterns.

(a)

(b)
Fig. 11 Co-pol and cross-pol E- (a) and H-plane (b) radiation patterns.

The measured E-plane co-pol and cross-pol patterns are shown in Fig. 11 (a). The simulated half power beamwidth is 35° which is well confirmed by measurement. A 37-dB isolation between the E-plane co-pol and cross-pol levels is measured in the main beam direction. Slight asymmetries in the patterns are attributed to the coaxial feed and attached cable which influence cross-pol performance. Fig. 11 (b) presents the measured and simulated H-plane co-pol and cross-pol patterns. The measured

H-plane half power beamwidth of 20° is in good agreement with the simulated value of 22°. The measured H-plane cross-polar levels are higher than the simulated ones, which is attributed to some metallic parts that could not be entirely covered by absorber material.

IV. CONCLUSION

An SIW H-plane horn antenna with approximately symmetric beam is proposed, designed and tested. The symmetric beam is achieved by the insertion of two rectangular slots in the top metallization of the H-plane horn antenna. Further measures have been taken to enhance front-to-back ratio and the 10-dB return-loss bandwidth. A reasonable compromise is achieved with narrow beamwidths in the two planes and improved bandwidth and front-to-back ratio. A bandwidth of approximately 600 MHz (4.62 %) with a reflection coefficient of 25.02 dB at 26.3 GHz is obtained. HPBWs of 35° and 20° are measured in E- and H-plane, respectively, with a gain of 11.6 dB. Good agreement between simulated and measured results is observed, thus validating the proposed antenna design.

REFERENCES

[1] M. Bozzi, L. Perredrini, K.Wu, and P. Arcioni, "Current and future research trends in substrate integrated waveguide technology," RadioEngineering, vol. 18, no. 2, pp. 201-209, Jun. 2009.

[2] K. Wu and D. Deslandes, "The substrate integrated circuits - A new concept for high-frequency electronics and optoelectronics," Proc. 6th Int. Conf. Telecom. Modern Satellite, Cable Broadcast. Serv., Nis, Yugoslavia, pp. III-X, Oct. 2003.

[3] W. Che, B. Fu, P. Yao, Y. L. Chow, and E. K. N. Yung, "A compact substrate integrated waveguide H-plane horn antenna with dielectric arc lens," Intl. J. RF Microw. Computer-Aided Engr., vol. 17, no. 5, pp. 473-479, Sep. 2007.

[4] L. Yu and Q. Shi-Wei, "A dielectric loaded H-plane horn for millimeter waves based on LTCC technology", Proc. Cross Strait Quad-Regional Radio Science Wirel. Technol. Conf., Chengdu, China, pp. 1-4, Jul. 2013.

[5] S. R. Ranade and D. U. Nair, "Design of substrate integrated waveguide H-plane horn antenna on a PTFE substrate for automotive radar application", Proc. Appl. Electromagn. Conf., Kolkata, India, pp. 1-4, Dec. 2011.

[6] N. Bayat-Makao and A. A. Kishk, "Substrate integrated horn antenna with uniform aperture distribution," IEEE Trans. Antennas Propagat., vol. 65, no. 2, pp. 514-520, Feb. 2017.

[7] M. Esmaeili and J. Bornemann, "Coaxial-fed dual-layer SIW horn antenna with improved E-plane radiation pattern," Proc. 47th Eur. Microw. Conf., Nuremberg, Germany, pp. 1-4, Oct. 2017 (in print).

[8] A. Patel, Alpesh Vala, R. Goswami, and K. Mahant, "Square loop slots loaded substrate integrated waveguide based horn antenna," Microw. Opt. Technol. Lett., vol. 58, no. 7, pp. 1577-1582, Jul. 2016.

[9] D. Deslandes and K. Wu, "Accurate modelling, wave mechanisms, and design considerations of substrate integrated waveguide," IEEE Trans. Microw. Theory Tech., vol. 54, no. 6, pp. 2516-2526, Jun. 2006.

[10] M. Esquius Morote, B. Fuchs, J. Zurcher, and J. Mosig, "A printed transition for matching improvement of SIW horn antennas," IEEE Trans. Antennas Propagat., vol. 61, no. 4, pp. 1923-1930, Apr. 2013.

[11] Y. Tang, Z. Wang, L. Xia, and P. Chen, "A novel high gain K-band H-plane SIW horn antenna using dielectric loading," Proc. Asia-Pacific Microw. Conf., Sendai, Japan, pp. 372-374, Nov. 2014.

[12] P. Benedek and P. Silvester, "Capacitance of parallel rectangular plates separated by a dielectric sheet," IEEE Trans. Microw. Theory Tech., vol. 20, no. 8, pp. 504-510, Aug. 1972.